

# Multi-Tailed Vision Transformer for Efficient Inference

Yunke Wang<sup>a</sup>, Bo Du<sup>a</sup>, Wenyuan Wang<sup>b</sup>, Chang Xu<sup>c</sup>

<sup>a</sup>*School of Computer Science, Wuhan University, Wuhan, China*

<sup>b</sup>*School of Electric Information, Wuhan University, Wuhan, China*

<sup>c</sup>*School of Computer Science, The University of Sydney, Sydney, Australia*

---

## Abstract

Recently, Vision Transformer (ViT) has achieved promising performance in image recognition and gradually serves as a powerful backbone in various vision tasks. To satisfy the sequential input of Transformer, the tail of ViT first splits each image into a sequence of visual tokens with a fixed length. Then, the following self-attention layers construct the global relationship between tokens to produce useful representation for the downstream tasks. Empirically, representing the image with more tokens leads to better performance, yet the quadratic computational complexity of self-attention layer to the number of tokens could seriously influence the efficiency of ViT's inference. For computational reduction, a few pruning methods progressively prune uninformative tokens in the Transformer encoder, while leaving the number of tokens before the Transformer untouched. In fact, fewer tokens as the input for the Transformer encoder can directly reduce the following computational cost. In this spirit, we propose a Multi-Tailed Vision Transformer (MT-ViT) in the paper. MT-ViT adopts multiple tails to produce visual sequences of different lengths for the following Transformer encoder. A tail predictor is introduced to decide which tail is the most efficient for the image to produce accurate prediction. Both modules are optimized in an end-to-end fashion, with the Gumbel-Softmax trick. Experiments on ImageNet-1K demonstrate that MT-ViT can achieve a significant reduction on FLOPs with no degradation of the accuracy and outperform other compared methods in both accuracy and FLOPs.

*Keywords:*

Vision Transformer, Efficient Inference, Dynamic Neural Network

---

## 1. Introduction

The great success of Transformer ([53, 11, 2]) in Natural Language Processing (NLP) has drawn computer vision researchers’ attention. There have been quite a few attempts on adopting the Transformer as an alternative deep neural architecture in computer vision. Vision Transformer (ViT) ([12]) is a seminal work that employs a fully Transformer architecture to address the image classification task. By first splitting an image into multiple local patches, ViT can then form a visual sequence for the Transformer input. The self-attention mechanism in ViT is capable of measuring the relationship between any two local patches and then information of patches are aggregated to produce a high-level representation for the image recognition task.

Following ViT, a number of variants ([68, 18, 4, 40, 52, 29, 71, 16, 55]) have been developed. For example, DeiT ([52]), without the pre-training on an extra large-scale dataset (*e.g.*, JFT-300M ([47])), for the first time boost ViT to achieve the state-of-the-art performance on the ImageNet-1K ([10]) benchmark. T2T-ViT ([68]), which can also be trained from scratch on the ImageNet-1K benchmark, proposes to boost the exchange of local information and global information with a T2T-module before the transformer encoder. CrossViT [4] exploits multi-scale features of the image in vision transformer and TNT [18] focuses on investigating the attention inside a single patch and propose the divide of a single patch into multiple smaller patches. CrossFormer [55] proposes a novel method that utilizes patches of different sizes to construct cross-scale attention, which shows great improvement in several important vision benchmarks. These efforts have thus ensured vision transformer to be a strong substitution (*i.e.*, Swin Transformer [37] and Twins [9]) for CNNs architecture [32, 20, 48] in vision tasks. However, compared with CNNs, vision transformers do not show a significant decrease in the computational cost, or sometimes consume even more.

As the computational cost of the transformer is quadratic to the sequence length, a natural idea is therefore to decrease the number of tokens in the transformer for a potential acceleration. But the number of tokens is also a key factor to the accuracy, which thus requests a non-trivial strategy of screening tokens to achieve a trade-off between accuracy and computational cost. Inspired by the pruning in CNNs [22], a few works suggest pruning tokens in vision transformers for efficient inference. PoWER-BERT [15] observes that the redundancy in Transformer gradually grows from the shallow layer to the high layer, and the token redundancy can be measured through their

attention scores. This insightful observation then motivated pruning methods that progressively prune tokens in vision transformers [45, 50, 6, 66, 64].

These pruning methods have shown great success in reducing the number of tokens for efficient inference in vision transformers, *i.e.*, all of them can preserve the accuracy under a nearly 40% FLOPs reduction. But their progressive pruning strategy only deals with the Transformer encoder, while leaving the very beginning number of tokens at the input of vision transformers untouched. In fact, the upper bound of the overall computational cost is mainly determined by the number of tokens in the “image-to-tokens” step before the Transformer encoder. If we split an image into fewer patches, there will be a shorter visual sequence input,

which implies a higher inference speed by the following vision transformer. Also, the different complexities of images will favor a customized number of patches to be split. An easy image could also be accurately recognized with fewer patches, while difficult images could need a more fine-grained split to guarantee the recognition accuracy, as shown in Figure 1.

This paper introduces the Multi-Tailed Vision Transformer (MT-ViT), a novel approach that optimizes the number of patches used to represent input images, thereby reducing computational cost. Unlike traditional Vision Transformers, which typically employ a single “tail” in their “image-to-tokens” module, MT-ViT incorporates multiple tails that can produce visual sequences of varying lengths. By projecting patches of corresponding resolution into the same d-dimensional token, we enable sharing of the subsequent Transformer encoder. When processing an input image, a tail predictor is trained to determine which tail should be used to generate the visual sequence. As tail selection is a non-differentiable process, we employ the Gumbel-Softmax technique to optimize MT-ViT and the tail predictor in an end-to-end fashion. We evaluate MT-ViT on both small scale

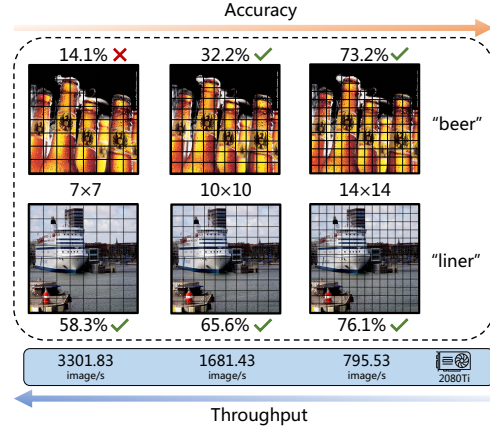


Figure 1: The throughput and confidence of prediction from DeiT-S, with a different number of tokens, *e.g.*,  $7\times 7$ ,  $10\times 10$  and  $14\times 14$ . The ‘tick’ and ‘cross’ sign denote the right and false prediction respectively.

datasets (*e.g.*, CIFAR100 [31], TinyImageNet [8]) and large scale datasets (*e.g.*, ImageNet-1K [10]) on top of various backbone (*e.g.*, DeiT [52], T2T-ViT [68] and MiniViT [69]). Empirical results show that MT-ViT can preserve the accuracy with an up to 70% reduction of FLOPs on CIFAR100 and TinyImageNet, and achieve an obvious advantage over comparison pruning methods on ImageNet-1K.

## 2. Related Work

In this section, we firstly discuss the development of vision transformer and then we introduce some efficient inference methods for vision transformer.

### 2.1. Vision Transformer

The transformer has been widely used in NLP community [53, 11, 2] and achieved great success. Inspired by this major success of transformer architectures in the field of NLP, researchers have recently applied transformer to computer vision (CV) tasks [17, 44, 21, 43, 42, 30, 70, 49, 19, 7, 27]. The early attempts about applying Transformer to vision tasks focus on combining convolution with self-attention. DETR [3] is proposed for object detection task, which first exploits the convolution layer to extract visual features and then refines features with Transformer. BotNet [46] replaces the convolution layers with multi-head self-attention layer at the last stage of ResNet [20] and achieves good performance.

ViT [12] is the first work to introduce a fully Transformer architecture directly into vision tasks. By pre-training on massive datasets like JFT-300M [47] and ImageNet-21K [10], ViT achieves state-of-the-art performance on various image recognition benchmarks. However, ViT’s performance is relatively modest when trained on mid-sized datasets such as ImageNet-1K [10]. In comparison to ResNet [20] of similar size, ViT obtains slightly lower accuracy. The primary reason for this discrepancy is that transformers lack certain inductive biases about images such as locality and translation equivariance. These biases are critical for generalization, particularly when training vision transformers with limited training data. Later, DeiT [52] manages to solve this data-efficient problem by simply modifying the Transformer and proposing a Knowledge Distillation (KD) [24] optimization strategy, with improved accuracy in ImageNet-1K. Some following work [68, 18, 4] focus on exploiting the local information of the image, which lead to a significantly

increasing performance. Also, some works [37, 40] try to adopt a deep-narrow structure like CNNs to produce multi-scale features for the downstream intensive prediction task. Since the vision transformer is known to suffer from a huge number of parameters, there are also some attempts to achieve parameter reduction while retaining the same performance [69, 61]. At present, vision transformer has dominated various vision tasks, such as medical image analysis [63, 62], hyperspectral data [65] and image generation [33, 28].

## 2.2. Efficient Transformer

Despite ViT’s impressive performance in vision tasks, achieving good performance requires significant computational resources. Consequently, researchers are interested in developing a more efficient Transformer architecture. Network pruning has been widely used in CNNs to speed up neural network inference (*i.e.*, filter pruning [22, 36, 51]) by formulating the pruning methods as decision-making problems [59, 58]. Some researchers [15, 45, 50, 6, 39, 64, 66, 35] have been inspired by this idea and have attempted to use token pruning to identify and eliminate inferior tokens in order to improve efficiency. More recently, A-ViT [66] achieves efficient computing by adaptively halting tokens that are deemed irrelevant to the task, thereby enabling dense computation only on the active informative tokens. This module reuses existing block parameters and utilizes a single neuron from the last dense layer in each block to compute the halting probability, requiring no additional parameters or computations. EViT [35] highlights the importance of class tokens and images by their attention scores. ATS [13] introduces a parameter-free module that scores and adaptively samples significant tokens. Some other approaches involve utilizing a pyramid structure to exploit multi-scale features and reduce overall computation, as demonstrated by PVT [54], HVT [40], and PiT [23].

The design of the pure vision transformer architecture is still a manually-crafted process. The optimal network depth, embedding dimension, and head number are still uncertain. To address this issue, some researchers are exploring the use of neural architecture search (NAS) [67, 41] to find an efficient ViT architecture. AutoFormer [5] combines the weights of various blocks in the same layers during supernet training. NASViT [14] aims to alleviate the gradient conflict issue in NAS and ensure the efficiency of the ViT model.

Some adaptive methods aim to reduce the inference time of the model conditionally [57]. Motivated by this idea, [1] proposes several multi-exit

architectures for dynamic inference in vision transformers. The core idea is to conduct an early exit in the middle layer when the prediction confidence is above the threshold. Dynamic-Vision-Transformer (DVT) [56] reduces the computational cost by considering cascading three Transformers with increasing numbers of tokens, which are sequentially activated in an adaptive fashion during the inference time. Specifically, an image is first sent into the Transformer with a fewer number of tokens. By investigating the prediction confidence, DVT decides whether to proceed to use the next Transformer. The subsequent model also considers utilizing the intermediate feature of the former Transformer.

### 3. Preliminaries

A standard Transformer in NLP tasks normally requires a 1D sequence of token embedding as the input. To handle 2D images, the tail of ViT splits an image  $X \in \mathbb{R}^{h \times w \times c}$  into  $N$  independent patches  $X_p$  in a  $p \times p$  resolution and then projects each local patch  $X_p$  into a  $d$  dimensions embedding to form a visual sequence  $Z_p \in \mathbb{R}^{N \times d}$ . Similar to BERT [11], ViT also introduces a learnable class token  $Z_{cls}$  into the input sequence (*i.e.*,  $Z = [Z_{cls}, Z_p]$ ). Subsequently, ViT learns a representation of the image with the following  $L$ -layers Transformer encoder, which mainly consists of two alternating components (*i.e.*, Multi-head Self-Attention (MSA) module and Multi-Layer Perceptron (MLP) module).

#### 3.1. Multi-head Self-Attention

MSA module calculates the relationship between any two tokens to generate the attention map  $A$  with self-attention layer. Given a sequential input  $Z \in \mathbb{R}^{(N+1) \times d}$ , standard self-attention module first projects  $Z$  linearly into three embedding called query  $\mathbf{Q}$ , key  $\mathbf{K}$  and value  $\mathbf{V}$  respectively,

$$[\mathbf{Q}, \mathbf{K}, \mathbf{V}] = ZW_{qkv}, \quad (1)$$

where  $W_{qkv} = [W_q, W_k, W_v] \in \mathbb{R}^{d \times 3d}$  denotes the linear projection operator. Then, the attention map  $A$  is calculated by the dot operation between query  $\mathbf{Q}$  and key  $\mathbf{K}$  and then the attention map  $A$  is finally applied to weight the value embedding  $\mathbf{V}$ . The whole process of self-attention can be defined as follows,

$$\text{SA}(\mathbf{Q}, \mathbf{K}, \mathbf{V}) = A\mathbf{V} = \text{softmax}\left(\frac{\mathbf{Q}\mathbf{K}^T}{\sqrt{d}}\right)\mathbf{V}. \quad (2)$$

Compared to the vanilla self-attention, multi-head self-attention runs  $k$  self-attention operations in parallel. The output of MSA can be formulated as follows,

$$\text{MSA}(\mathbf{Q}, \mathbf{K}, \mathbf{V}) = \text{Concat} \left[ \text{softmax} \left( \frac{\mathbf{Q}^h \mathbf{K}^{hT}}{\sqrt{d}} \right) \mathbf{V}^h \right]_{h=1}^H. \quad (3)$$

### 3.2. Multi-Layer Perceptron

The MLP module is applied after MSA module for representing feature and introducing non-linearity. Denoting  $Z'$  as the output of MSA module, MLP can be defined as follows,

$$\text{MLP}(Z') = \phi(Z' W_{fc}^a) W_{fc}^b, \quad (4)$$

where  $W_{fc}^a$  and  $W_{fc}^b$  denote the fully-connected layer, and  $\phi$  denotes the non-linear activate function (*e.g.*, GELU).

### 3.3. Transformer Encoder

The Transformer encoder is constructed by stacking MSA module and MLP module with residual connection. Therefore, the encoder can be defined as

$$Z'_l = Z_{l-1} + \text{MSA}(\text{LN}(Z_{l-1})), \quad (5)$$

$$Z_l = Z'_l + \text{MLP}(\text{LN}(Z'_l)), \quad (6)$$

where  $\text{LN}(\cdot)$  is the layer normalization for stable the training of Transformer.

### 3.4. Analysis of the computation complexity

The floating-point operations (FLOPs) is commonly used as a metric to measure the theoretical computational cost of the model. After summing up the FLOPs of all the operations in the Transformer encoder, we find that MSA and MLP contribute the most to FLOPs. Specifically, the FLOPs of MSA are  $4Nd^2 + 2N^2d$  and the FLOPs of MLP are  $2Nd^2r$ , where  $r$  is the dimension expansion ratio of the fully-connected layer in MLP. From the analysis above, we can observe that the FLOPs of the Transformer encoder is quadratic to the embedding dimension  $d$  and number of tokens  $N$ . Due to the large number of  $d$  and  $N$  (usually hundred), the computational cost of vision transformer is large. However, if we reduce these two hyper-parameters

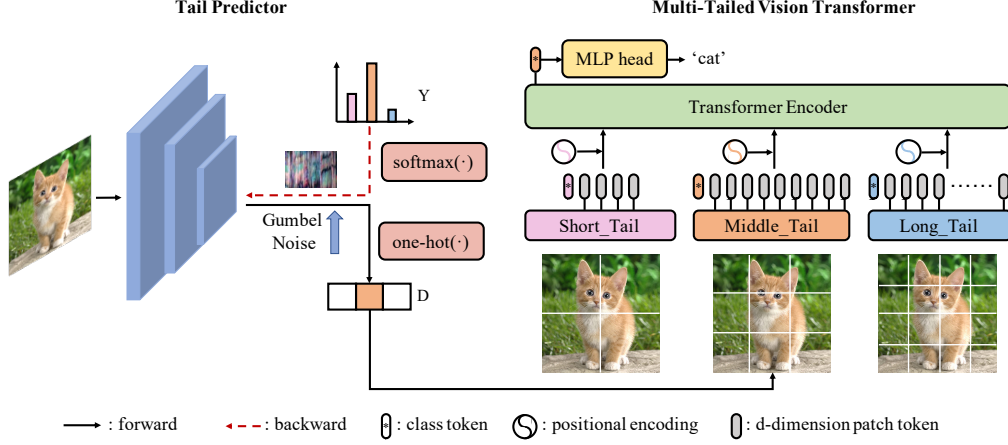


Figure 2: The framework of proposed method contains two main components: scale predictor  $\pi_\theta$  and multi-tailed vision transformer (MT-ViT). The number of scale  $K$  is set to 3. (a) The tail predictor is a CNN-based model which decides which tail is suitable for the image. (b) By using the multiple tails in MT-ViT, patches with different sizes are all projected into a  $d$  dimension embedding. This makes it possible to share the Transformer encoders and MLP head.

for ViT model, we can easily obtain a rapidly decrease in computational cost without modifying the architecture of the Transformer.

Adjusting the embedding dimension  $d$  has been well considered in various ViT backbones. By setting  $d$  from a small value to a large value, we can obtain ViT model with increasing FLOPs (*i.e.*, ViT-Small, ViT-Base and ViT-Large). In return for the high complexity, the larger the model size is, the higher accuracy the model will normally achieve. Another way is to consider the number of tokens  $N$ , which can be up to the resolution of the local patch. For an image of  $224 \times 224$  size, ViT model normally splits the image into non-overlap patches with  $16 \times 16$  size, so the number of tokens  $N$  is equal to  $(224/16)^2 = 196$ . By setting different patch resolutions, we can obtain different ViT models, *e.g.*, ViT-Base/14, ViT-Base/16 and ViT-Base/32.

#### 4. Methodology

While vision transformer achieves promising performance in vision tasks, how to reduce its increasing computational cost for efficient inference draws great attention to researchers. As discussed in Section 3, decreasing the



number of tokens  $N$  can be an effective way to ensure a significant reduction on FLOPs. Pruning methods have been investigated in Transformer [45, 50] to screen out uninformative tokens at the middle layer. However, there could still be possible for a greater reduction of computational cost by reducing the number of tokens at the earlier position. Based on this idea, we further consider reducing tokens at the “image-to-tokens” step for a potential FLOPs reduction in this paper.

In the “image-to-tokens” step before the Transformer, an image  $X \in \mathbb{R}^{h \times w \times c}$  is decomposed into a sequence of non-overlap patches with  $p \times p$  size and the number of patches  $N$  is equal to  $(h \times w)/p^2$ . Therefore, the resolution of the local patch can determine the length of the visual sequence and further affects the accuracy and computational cost of ViT. With a fine-grained patch size, ViT could reach higher performance with increasing FLOPs. On the contrary, with a coarse-grained patch size, the performance of ViT decreases with a reduction of FLOPs.

Motivated by this idea, we consider leveraging the advantages of both fine-grained patch size and coarse-grained patch size to achieve the trade-off between accuracy and efficiency. Intuitively, easy images could be accurately recognized with a coarse-grained patch size while difficult images often require a fine-grained patch split to achieve an accurate prediction. To achieve this, we firstly need a network module that can be compatible with both fine-grained patch and coarse-grained patch. A natural idea is to construct a stack of  $K$  independent vision transformers  $F(X) = [f_1, f_2, \dots, f_K]$ , which are pre-trained with its corresponding  $K$  patch sizes (*i.e.*,  $p_1, p_2, \dots, p_K$ ). To decide which Transformer is suitable for the image, a one-hot decision vector  $D \in [0, 1]^K$  is introduced to determine which patch size  $p$  is proper for the given image. With an optimal decision  $D$ , we can minimize computational cost as far as possible while preserving the accuracy of the model.

The basic workflow is illustrated as follows. Denoting  $m$  as the number of classes and  $f_k(X) \in \mathbb{R}^m$  as the logit of the  $k$ -th stacked ViT model, the final prediction of the whole stacked model  $\hat{F}$  is the sum of each Transformer with weight  $D$ , which can be formulated as

$$\hat{F}(X) = D \odot F(X) = \sum_{i=0}^K D_i f_i(X). \quad (7)$$

The classification loss  $L_{\text{cls}}$  for image  $X$  can be written as

$$L_{\text{cls}} = \text{Cross\_Entropy}(\hat{F}(X), Y_{\text{cls}}), \quad (8)$$

where  $\text{Cross\_Entropy}(\cdot)$  is the softmax cross-entropy loss and  $Y_{\text{cls}}$  is the class label related to  $X$ .

#### 4.1. Multi-Tailed Vision Transformer

In the stacked Transformer framework, a stack of  $K$  independent vision transformers is used to process multi-scale visual sequences respectively. But the stacked Transformers directly lead to a  $K$  times number of parameters than that of a single vision transformer model, which is horribly parameter-inefficient. Normally, setting some shared parameters and layers among these independent Transformers is essential for reducing the parameter of the model when processing multi-scale input.

Inspired by this idea, we adopt a shared Transformer encoder in the stacked Transformer  $F$ , which results in the multi-tailed vision transformer (MT-ViT). The “image-to-tokens” step is referred as the tail of ViT. MT-ViT adopts  $K$  independent tails for projecting patches in different sizes into a  $d$ -dimension embedding, and then shares all parameters of Transformer encoders and classification head, as shown in Figure 2. The instance-aware tails are conditioned to images and projects patches of different sizes into vectors of the same dimension to satisfy the input requirement of the public Transformer encoder. As the inside architecture of Transformer encoder has not been changed, we can make MT-ViT serve as a general backbone that is compatible with the mainstream ViT backbones.

MT-ViT adopts multiple tails before the Transformer encoder. For the  $i$ -th tail, it should receive patches  $x_p$  of size  $p_i$  and then proceed  $x_p$  into the projection function  $\mathcal{T}_i(\cdot)$  to get the embedding  $z_i$ , where  $z_i = \mathcal{T}_i(x_p) \in \mathbb{R}^d$ . For different vision transformer backbones, the projection function  $\mathcal{T}$  can be quite different, therefore we should re-design the tail to produce dynamic sequences of  $d$ -dimension embedding when MT-ViT is equipped with different ViT backbones. Please refer to the experimental part for more details.

#### 4.2. Dynamic Tail Selection

Optimizing MT-ViT (Eq. (8)) could be intractable for the following reason. In the classical image classification task, images and their corresponding label are the only available information in the training set, while the optimal tail selection  $D$  remains unknown. We therefore expect an appropriate estimation on decision  $D$ , so that we can well indicate the “easiness” of the image and make full use of the multi-tailed vision transformer backbone. To

solve this problem, we propose a CNN-based tail predictor  $\pi_\theta$  to automatically distinguish the “easiness” of the image and output the proper decision  $D$ . Given the image  $X$ , the policy  $\pi_\theta$  outputs the categorical distribution,

$$\zeta = [\zeta^{(1)}, \zeta^{(2)}, \dots, \zeta^{(K)}] = \pi_\theta(X), \quad (9)$$

where  $\zeta^{(i)}$  represents the probability of choosing the  $i$ -th patch size. To generate decision  $D$ , we need to sample from  $\zeta$  or select the highest probability of  $\zeta$  to get the one-hot vector. However, both sampling from softmax distribution and selecting the highest value in  $\zeta$  are non-differentiable, which precludes the back-propagation and impedes the end-to-end training.

#### 4.2.1. Differentiable Tail Sampling

To overcome this problem, we apply the Gumbel-Softmax trick [26] to form a Gumbel-Softmax distribution and transform the soft probability  $\zeta$  to a discrete variable  $D \in \{0, 1\}^K$  as follows,

$$D = \text{one\_hot}\left(\arg \max_i [g^{(i)} + \log \zeta^{(i)}]\right) \quad (10)$$

where  $g^{(1)}, \dots, g^{(k)}$  are *i.i.d* random noise samples drawn from Gumbel(0, 1) distribution. The Gumbel distribution has shown to be stable under max operations [38]. By applying the inverse-CDF transformation,  $g^{(i)}$  can be computed as

$$g^{(i)} = -\log(-\log(u^{(i)})), \quad u^{(i)} \sim U(0, 1), \quad (11)$$

where  $U(0, 1)$  is the Uniform distribution. Since the  $\arg \max(\cdot)$  in Eq. (10) is still a non-differentiable operation, we further use the softmax function as a continuous, differentiable approximation to replace  $\arg \max(\cdot)$ . A differentiable sampling  $Y = [y^{(1)}, y^{(2)}, \dots, y^{(K)}] \in \{0, 1\}^K$  can be written as,

$$y^{(i)} = \frac{\exp(\log \zeta^{(i)} + g^{(i)})/\tau}{\sum_{i=1}^m \exp[(\log \zeta^{(i)} + g^{(i)})/\tau]}, \quad i = 0, 1, \dots, K, \quad (12)$$

where  $\tau \in (0, +\infty)$  is the temperature parameter to adjust the Gumbel-Softmax distribution.  $Y$  can be regarded as continuous relaxations of one-hot vectors  $D$ . As the softmax temperature  $\tau$  approaches 0, samples from the Gumbel-Softmax distribution approximate one-hot vectors. The sampling of

the approximated one-hot vector is refactored into a deterministic function-componentwise addition followed by  $\arg \max$  of the parameters  $\log \zeta$  and fixed Gumbel distribution  $-\log(-\log(u))$ . The non-differentiable part is therefore transferred to the samples  $g$  from the Gumbel distribution. This reparameterization trick allows gradients to flow from decision  $D$  to the  $\theta$  and both tail predictor and MT-ViT can be optimized as a whole with Eq. (8).

However in our setting, we are constrained to sample discrete values strictly because we can only choose one tail of MT-ViT to make the prediction. Inspired by Straight-Through Gumbel Estimator, in the forward propagation, we discretize  $D$  using  $\arg \max(\cdot)$  in Eq. (10) but use the continuous approximation in the backward propagation by approximating  $\nabla_{\theta} D \approx \nabla_{\theta} Y$ .

#### 4.2.2. Optimization

The basic loss function (Eq. (8)) defines a softmax cross-entropy loss between the prediction of MT-ViT and the ground-truth label. The multi-tailed vision transformer backbone and the tail predictor are optimized jointly with the Gumbel-Softmax trick. However, Eq. (8) only considers achieving better accuracy, which makes the tail predictor always encourage MT-ViT to activate the tail with the highest accuracy and therefore lead to the collapse of the predictor’s training. To solve this problem, we consider adding a FLOPs constraint regularization on the choice of different tails. The total loss can be written as follows,

$$L_{\text{total}} = L_{\text{cls}} + \lambda L_f \quad (13)$$

where  $L_f$  is the FLOPs regularization and  $\lambda$  is the hyper-parameter to achieve the trade-off between accuracy and FLOPs. The FLOPs regularization can punish the situation when the predictor selects the tail with high computational cost. On the contrary, in those situations where the predictor selects the tail with low FLOPs, the regularization should not contribute any penalty to the total loss. In this spirit, our designed FLOPs constraint regularization is formulated as follows

$$L_f = \max \left( \alpha, \sum_{i=0}^K D_i c_i \right) - \alpha, \quad (14)$$

where  $c_i$  is the normalized FLOPs of the  $i$ -th branch and  $\alpha$  is the hyper-parameter to adjust the threshold of penalty. While the FLOPs of the selected model is larger than the threshold  $\alpha$ ,  $L_f$  will punish the prediction.

### 4.3. Discussion

#### 4.3.1. The idea of adjusting patch size

The idea of adjusting the patch size for efficiency has been investigated in some related works, such as Swin Transformer [37]. Swin Transformer progressively merges local patches as the network gets deeper. Compared to Swin Transformer, we highlight the novelty of MT-ViT as follows. First, Swin Transformer adjusts the patch size of the image at the middle layer of the transformer. There could still be possible for a greater reduction of computational cost by adjusting the patch size at the earlier position. Hence, we propose several tail modules before the transformer encoder to divide the image with different patch sizes at the very beginning. A tail predictor is proposed to automatically assign images to different tails and achieve the trade-off between accuracy and computational cost. Second, Swin Transformer treats all samples equally and there is no patch size selection step for each individual image. By contrast, we adopt a tail predictor to conduct dynamic selection for each image in MT-ViT. Easy images are split into shorter sequences while difficult images are split into longer sequences. This dynamic process enhances the efficiency compared to simply treating all samples as equal.

#### 4.3.2. Dynamic tail selection and multi-resolution tokens

Extra predictors with Gumbel-Softmax selection have been investigated in some related works like DynamicViT [45]. Compared to DynamicViT, the predictor in MT-ViT appears in different positions. In DynamicViT, the predictor is set to be in the middle layer, while the predictor in MT-ViT is placed at the beginning of the transformer. This design could keep the original architecture of the transformer as a whole and therefore makes it easier to switch from different backbones. The idea of multi-resolution tokens has also been used in DVT [56] and we will discuss the empirical results between DVT and MT-ViT in the experiment.

## 5. Experiment

In this section, we conduct extensive experimental analysis on the small-scale datasets, CIFAR100 [31] and TinyImageNet [8], and large-scale dataset, ImageNet-1K benchmark [10] to show the performance of our proposed Multi-Tailed Vision Transformer in various aspects.

Table 1: Detailed information of datasets used for training.

Dataset	Train size	Val size	Classes	Size
CIFAR100	50,000	10,000	100	$32 \times 32$
TinyImageNet	100,000	10,000	100	$64 \times 64$
ImageNet	1,281,167	50,000	1,000	N/A

## 5.1. Experiment Setting

### 5.1.1. Datasets

CIFAR100 [31] is a widely-used dataset for image recognition tasks, which contains 50,000 training images and 10,000 test images. There are 100 classes in this dataset, grouped into 20 superclasses. Each image has a “fine label” as the class label and a “coarse label” as the superclass. In our experiment, we only make use of fine labels. TinyImageNet [8] is a subset of the well-known ImageNet-1K benchmark, which contains 100,000 images with  $64 \times 64$  resolution with 100 categories. ImageNet-1K [10] is the most popular benchmark to evaluate the classification performance of the deep learning model. It contains 1.28 million training images and 50,000 validation images with 1000 categories. Details of these three datasets are summarized in Table 1.

### 5.1.2. Backbones

We implement MT-ViT on top of two popular ViT backbones (*i.e.*, DeiT-Ti/S [52] and T2T-ViT-7/12 [68]). As for the tail predictor, we choose the light-weight MobileNetv3-small [25] as the backbone since we want to minimize the computational influence of scale predictor to the whole framework as far as possible. The number of parameters and FLOPs of MobileNetv3-small is 2.54M and 0.06G, respectively. Followed with DVT [56], MT-ViT employs three tails, *i.e.*, Short Tail (ST), Middle Tail (MT) and Long Tail (LT), to output different numbers of tokens, *i.e.*,  $7 \times 7$ ,  $10 \times 10$ ,  $14 \times 14$ . For DeiT, a convolutional kernel with  $p \times p$  size and  $p$  stride can be used to create non-overlap tokens. So for a  $224 \times 224$  image, we can obtain  $7 \times 7$ ,  $10 \times 10$  and  $14 \times 14$  tokens by setting  $p$  to 32, 23 and 16 in different tails. Notice that for the middle tail, the images should be firstly resized to  $230 \times 230$  resolution.

As for T2T-ViT, the T2T module is used to produce a sequence of tokens. The three soft split procedures are mainly responsible for controlling the number of tokens in T2T-ViT. In each soft split, the patch size is  $p \times p$  with  $s$  overlapping and  $k$  padding on the image, where  $p - s$  is similar to the stride in convolution operation. So for an image  $X \in \mathbb{R}^{h \times w \times c}$ , the number of

Table 2: The Design and FLOPs of each tail in MT-ViT.

Backbone	Patch Embedding	FLOPs(G)		
		ST	MT	LT
T2T-ViT-7	T2T-module	0.3	0.55	1.1
T2T-ViT-12	T2T-module	0.33	0.7	1.78
DeiT-Ti	Convolution	0.31	0.61	1.25
DeiT-S	Convolution	1.14	2.3	4.6
DeiT-B	convolution	4.41	8.9	17.6

Table 3: The performance of MT-ViT in CIFAR100 and TinyImageNet.  $\eta$  and  $\alpha$  are set to 0.25, 0.75 for MT-ViT(A\*), and 1, 0.25 for MT-ViT(S\*).

Backbone	Method	CIFAR100		TinyImageNet	
		Top-1 Acc.(%)	FLOPs.(G)	Top-1 Acc.(%)	FLOPs.(G)
T2T-ViT-7	MT-ViT(A*)	82.8(+1.1)	0.71(-35.2%)	86.6(+1.6)	0.93(-15.9%)
	MT-ViT(S*)	81.8(+0.1)	0.49(-55.9%)	85.1(+0.1)	0.57(-48.2%)
	Baseline	81.7	1.1	85.0	1.1
T2T-ViT-12	MT-ViT(A*)	85.7(+2.2)	1.17(-34.2%)	90.0(+1.5)	1.41(-21.0%)
	MT-ViT(S*)	84.0(+0.5)	0.53(-70.4%)	88.6(+0.1)	0.85(-58.5%)
	Baseline	83.5	1.8	88.5	1.8
DeiT-Ti	MT-ViT(A*)	84.9(+2.0)	0.78(-37.2%)	88.8(+2.1)	0.99(-20.86%)
	MT-ViT(S*)	83.4(+0.5)	0.47(-62.0%)	86.7(+0.0)	0.47(-64.0%)
	Baseline	82.9	1.3	86.7	1.3
DeiT-Small	MT-ViT(A*)	87.9(+0.9)	2.59(-43.6%)	94.3(+1.4)	3.18(-31.0%)
	MT-ViT(S*)	87.0(+0.0)	1.2(-72.0%)	93.5(+0.6)	2.21(-52.0%)
	Baseline	87.0	4.6	92.9	4.6

output tokens  $N$  after soft split is

$$N = \lfloor \frac{h + 2k - p}{p - s} + 1 \rfloor \times \lfloor \frac{w + 2k - p}{p - s} + 1 \rfloor. \quad (15)$$

In the long tail, the patch size for the three soft splits is  $p = [7, 3, 3]$ , and the overlapping is stride  $s = [3, 1, 1]$ , which reduces the size of the input image from  $224 \times 224$  to  $14 \times 14$ . By setting  $s = [5, 1, 1]$  and  $p = [11, 3, 3]$ , the middle tail can produce  $10 \times 10$  tokens. By setting  $s = [7, 1, 1]$  and  $p = [14, 3, 3]$ , the short tail can produce  $7 \times 7$  tokens. Therefore, we can adopt multiple tails and obtain MT-ViT backbone. The FLOPs of each branch is given in Table 2.

### 5.1.3. Implementation Details

The whole training mainly contains two processes. We first pre-train the MT-ViT backbone and then jointly finetune both tail predictor and MT-ViT

in an end-to-end fashion. In the backbone pre-training, all tails are activated and the loss is a sum of all three tails’ losses. The pre-training setting is basically the same as that in the official implementation of DeiT and T2T-ViT. We pre-train the MT-ViT backbone for 300 epochs on ImageNet-1K. For small-scale experiments, we transfer the pre-trained MT-ViT backbone to the downstream datasets such as CIFAR100 and TinyImageNet. Following the implementation of T2T-ViT, we finetune the pre-trained MT-ViT backbone for 60 epochs by using an SGD optimizer and cosine learning rate decay. When it comes to the finetune step, a tail predictor is introduced to determine which tail is suitable for the image. We jointly finetune the MT-ViT backbone and the predictor for 30 epochs.

#### 5.1.4. Metric

The reported FLOPs considers both tail predictor and MT-ViT. Supposing  $f_{st}$ ,  $f_{mt}$  and  $f_{lt}$  are the FLOPs of three tails, the overall FLOPs is calculated by  $\frac{(f_{st} \times n_{st} + f_{st} \times n_{mt} + f_{st} \times n_{lt})}{(n_{st} + n_{mt} + n_{lt})} + f_{predictor}$ , where  $n_{st}$ ,  $n_{mt}$  and  $n_{lt}$  are numbers of images that have been processed by each individual tail and  $f_{predictor}$  is the FLOPs of the tail predictor.

#### 5.2. Experiment on Small-Scale Datasets

We first conduct small-scale experiments on CIFAR100 and TinyImageNet. We implement MT-ViT on four versions of DeiT/T2T-ViT backbones, *i.e.*, DeiT-Ti, DeiT-S, T2T-ViT-7 and T2T-ViT-12. The experimental results are shown in Table 3. MT-ViT(A\*) and MT-ViT(S\*) are the same methods but they use different  $\eta$  and  $\alpha$  to adjust the trade-off between accuracy and speed. The former aims to achieve higher accuracy while the latter pursues a lower computational cost.

Compared to the baseline, it can be clearly observed that MT-ViT(A\*) can outperform the baseline by 1%-2% while still keeping a visible advantage on FLOPs in both CIFAR100 and TinyImageNet datasets. For example, MT-ViT(A\*) achieves 82.8%, 85.7%, 84.9%, and 87.9% on CIFAR100 with four ViT backbones, which gains an improvement of 1.1%, 2.2%, 2.0% and 0.9% over baseline, respectively. With this clear advantage in accuracy, we can still witness a decline in FLOPs of MT-ViT(A\*), which is 35.2%, 34.2%, 37.2%, and 43.6%. The same thing happens in TinyImageNet. MT-ViT(A\*) has roughly the same improvement in accuracy while retaining a 15%-30% reduction in computational cost with four ViT backbones. By contrast, MT-ViT(S\*) retains a similar accuracy with baseline but it has a significant



reduction in FLOPs. For instance, MT-ViT(S\*) implemented on top of DeiT-S has a similar accuracy of 87.0% in CIFAR100 datasets, however, there is a significant decline (over 70%) in the computational cost compared to the baseline.

### 5.3. Experiment on Large-Scale Datasets

In the following experiments, we investigate the performance of MT-ViT on large-scale benchmark ImageNet-1K. We build MT-ViT with three backbones, *i.e.*, DeiT-Ti, DeiT-S and T2T-ViT-12.

#### 5.3.1. Compared Methods

We compare our method with several state-of-the-art methods including model pruning methods and ViT-based methods that consider exploiting multi-scale features. SCOP [51] is the state-of-the-art method in pruning the channel of CNNs. Inspired by this, we re-implement it to reduce the patches in vision transformers. PoWER [15] accelerates BERT’s inference by progressively pruning tokens in BERT’s layer. We directly transfer PoWER from BERT to vision transformer. DynamicViT [45], PS-ViT [50], SViTE [39], Evo-ViT [64], IA-RED<sup>2</sup> [39] and EViT [34] are six highly related compared methods that consider accelerating the inference by progressively pruning tokens of the middle layer with self-slimming or a gate function. DVT [56] considers to cascade multiple vision transformer with adaptive sequence and conducts early-exit for acceleration. CrossViT [4] and HVT [40] are compared since they also consider using different scale features of images to adopt an efficient vision transformer.

#### 5.3.2. Performance

The results are shown in Table 4. Since SCOP [51] is designed for the pruning in the CNNs model, it is not surprising that SCOP does not perform quite well in this migration. Though there is an approximating 40% reduction on the FLOPs, its accuracy drops rapidly as well (*i.e.*, -3.3% in DeiT-Ti and -2.3% in DeiT-S). PoWER [15] performs only slightly better than SCOP, which suggests that the Transformer pruning in NLP fields is not the optimal solution for the vision transformer. By contrast, the pruning methods designed for vision transformer, *i.e.*, PS-ViT [50], SViTE [39], DynamicViT [45], Evo-ViT [64], IA-RED<sup>2</sup>[39] and EViT [34], are significantly better. For example, all these three methods can decrease the FLOPs up to 40% in DeiT-S, with a small reduction of accuracy (less than 0.7%).

Table 4: Main results of MT-ViT and other compared methods with three different ViT backbones on ImageNet-1K benchmark.

Backbone	Method	Top-1 Acc.(%)	Top-5 Acc.(%)	FLOPs(G)	FLOPs↓(%)
DeiT-Ti	Baseline	72.2	91.1	1.3	0
	SCOP[51] (NeurIPS, 2020)	68.9(-3.3)	89.0(-2.1)	0.8	-38.5
	PoWER[15] (ICML, 2020)	69.4(-2.8)	89.2(-1.9)	0.8	-38.5
	HVT-Ti[40] (ICCV, 2021)	69.6(-2.6)	89.4(-1.7)	0.7	-46.2
	SViT[6] (NeurIPS, 2021)	71.8(-0.4)	90.8(-0.3)	1.0	-23.1
	DynamicViT- $\rho/0.7$ [45] (NeurIPS, 2021)	71.0(-1.2)	90.4(-0.7)	0.8	-38.5
	DynamicViT- $\rho/0.9$ [45] (NeurIPS, 2021)	72.3(+0.1)	91.2(+0.1)	1.0	-23.1
	Evo-ViT[64] (AAAI, 2022)	72.0(-0.2)	91.0(-0.1)	0.8	-38.5
	PS-ViT[50] (CVPR, 2022)	72.0(-0.2)	91.0(-0.1)	0.7	-46.2
	A-ViT[66] (CVPR, 2022)	71.0(-0.2)	90.4(-0.7)	0.8	-38.5
	MT-ViT (Ours)	<b>72.9(+0.7)</b>	<b>91.3(+0.2)</b>	0.8	-38.5
DeiT-Small	Baseline	79.8	95.0	4.6	0
	SCOP[51] (NeurIPS, 2020)	77.5(-2.3)	93.5(-1.5)	2.6	-43.6
	PoWER[15] (ICML, 2020)	78.3(-1.5)	94.0(-1.0)	2.7	-41.3
	HVT-S[40] (ICCV, 2021)	78.0(-1.8)	93.8(-1.2)	2.4	-47.8
	PS-ViT[50] (CVPR, 2022)	79.4(-0.4)	94.7(-0.3)	2.6	-43.5
	SViT[6] (NeurIPS, 2021)	79.2(-0.6)	94.5(-0.5)	3.0	-34.8
	IA-RED <sup>2</sup> [39] (NeurIPS, 2021)	79.1(-0.7)	94.5(-0.5)	3.2	-30.4
	DynamicViT- $\rho/0.7$ [45] (NeurIPS, 2021)	79.3(-0.5)	94.7(-0.3)	2.9	-37.0
	DynamicViT- $\rho/0.9$ [45] (NeurIPS, 2021)	79.8(-0.0)	<b>94.9(-0.1)</b>	4.0	-13.0
	Evo-ViT[64] (AAAI, 2022)	79.4(-0.4)	94.8(-0.2)	3.0	-34.8
	EViT[64] (ICLR, 2022)	79.5(-0.3)	94.8(-0.2)	3.0	-34.8
	ATS[13] (ECCV, 2022)	79.7(-0.2)	94.9(-0.1)	2.9	-37.0
	MT-ViT(S*) (Ours)	79.5(-0.3)	94.4(-0.6)	2.5	-45.7
	MT-ViT(A*) (Ours)	<b>80.3(+0.5)</b>	<b>94.9(-0.1)</b>	3.5	-23.9
DeiT-Base	Baseline	81.8	95.6	17.6	0
	SCOP[51] (NeurIPS, 2020)	79.7(-2.1)	94.5(-1.1)	10.2	-42.0
	PoWER[15] (ICML, 2020)	80.1(-1.7)	94.6(-1.0)	10.4	-39.2
	DynamicViT- $\rho/0.7$ [45] (NeurIPS, 2021)	81.3(-0.5)	95.3(-0.3)	11.5	-35.0
	DynamicViT- $\rho/0.9$ [45] (NeurIPS, 2021)	<b>81.8(-0.0)</b>	95.5(-0.1)	15.5	-14.0
	MT-ViT(Ours)	<b>81.8(-0.0)</b>	<b>95.6(-0.0)</b>	13.9	-21.0
T2T-ViT-12	Baseline	76.5	93.5	1.8	0
	PoWER[15] (ICML, 2020)	74.5(-2.0)	92.6(-0.9)	1.2	-32.6
	DynamicViT- $\rho/0.7$ [45] (NeurIPS, 2021)	76.1(-0.4)	93.1(-0.4)	1.2	-32.6
	DynamicViT- $\rho/0.9$ [45] (NeurIPS, 2021)	76.8(+0.3)	93.5(-0.0)	1.5	-16.7
	MT-ViT (Ours)	<b>77.2(+0.7)</b>	<b>93.7(+0.2)</b>	1.5	-16.7

Our MT-ViT performs even better than these two methods, which achieves a similar FLOPs reduction but reaches higher accuracy. For example, with DeiT-Ti model, a nearly 40% reduction in FLOPs makes MT-ViT comparable with other comparison methods in the computational cost. However, MT-ViT can outperform the baseline by 0.7% in Top-1 accuracy and 0.2% in Top-5 accuracy while other competing methods are clearly below the baseline. When running in a high-speed mode with the DeiT-S model, the accuracy and FLOPs of MT-ViT are comparable with other methods. When it comes to the high-accuracy mode, MT-ViT can outperform competing methods at least 0.5%.

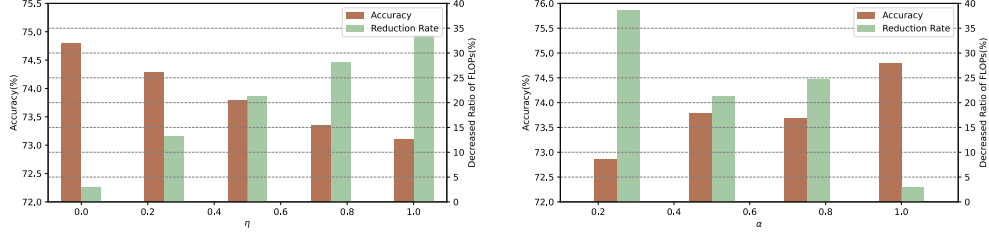


Figure 3: Ablation study on the hyper-parameter  $\alpha$  and  $\eta$  in FLOPs regularization term.  $\alpha$  is fixed to 0.5 in the left figure and  $\eta$  is fixed to 0.5 in the right figure.

### 5.3.3. Influence of $\alpha$ and $\eta$

We also investigate how the hyper-parameter  $\eta$  and  $\alpha$  in FLOPs constraint regularization would influence the performance of MT-ViT. The results are shown in the Figure 3. In the left figure, we maintain a fixed value of  $\alpha$  (0.5) and vary the values of  $\eta$  from 0 to 1. Conversely, in the right figure, we keep  $\eta$  fixed at 0.5 and adjust  $\alpha$  in the range of 0.25 to 1. We can clearly observe a trend that when setting a larger value for  $\eta$  and a smaller value for  $\alpha$ , we generally observe a decrease in accuracy accompanied by an increase in FLOPs reduction. By setting different  $\eta$  and  $\alpha$ , we can achieve different trade-offs for MT-ViT.

### 5.3.4. Relative Positional Encoding

As shown in Figure 2, MT-ViT is equipped with absolute position encoding. Adding relative positional encoding to the transformer encoder is an interesting idea and worth to be investigated. We re-implement MT-ViT backbone and add iPRE [60] as relative position encoding. Table 7 presents a comparison between MT-ViT with and without iPRE as the relative position encoding. The findings demonstrate that the inclusion of iPRE yields remarkable improvements. Specifically, MT-ViT with iPRE showcases a noteworthy increase in accuracy, achieving a gain of +0.3%. Remarkably, this advancement comes hand in hand with a substantial reduction in FLOPs, achieving an impressive decrease of 46.2%.

### 5.3.5. Compare with DVT and MiniViT

DVT is a great method for efficient inference in vision transformer. By adjusting the confident threshold of output logits, the trade-off of DVT between accuracy and FLOPs can be flexible. To provide a thorough comparison with

Table 5: Performance of MT-ViT when equipped with different ways of position encoding (PE).

PE	Method	Top-1 Acc.(%)	FLOPs(G)
Absolute	DeiT-Ti	72.2	1.3
	MT-ViT	<b>72.9(+0.7)</b>	<b>0.8(-38.5%)</b>
Relative	DeiT-Ti	72.7	1.3
	MT-ViT	<b>74.0(+0.3)</b>	<b>0.7(-46.2%)</b>

DVT, we draw a FLOPs-Accuracy curve to compare the performance of both methods, which are based on DeiT-Small.

From the figure, we can observe that when running in a relatively lower FLOPs mode (less than 2.5G), MT-ViT achieves a higher accuracy than DVT. When running in a high FLOPs mode, the accuracy of DVT tends to be higher than MT-ViT. This could be attributed to the large number of parameters in DVT, which enables a stronger backbone after pre-training. However, obtaining such a backbone should also require additional computational costs.

First, the number of parameters in DVT is much larger than MT-ViT. For DeiT-S, the number of DVT’s parameters is 70.4M, which is around 3 times more than that of the vanilla DeiT-S (22M) and that of MT-ViT (24.5M). This could require large memory during the training and inference. Second, the training cost of DVT is much higher than MT-ViT. The training speed for DVT and MT-ViT is 751.86 img/s and 1864.87 img/s respectively. Since both methods need to pre-train the backbone for 300 epochs, it is clear that DVT requires significantly more computational resources. Based on the results and analysis above, we think MT-ViT is a better choice than DVT in practice, especially when the computation resources are limited.

MiniViT [69] is a great ViT method, which can significantly reduce the model size. From Table 6, we can observe that MiniViT can reduce the parameter size of the model by 50% and there is no reduction in the compu-

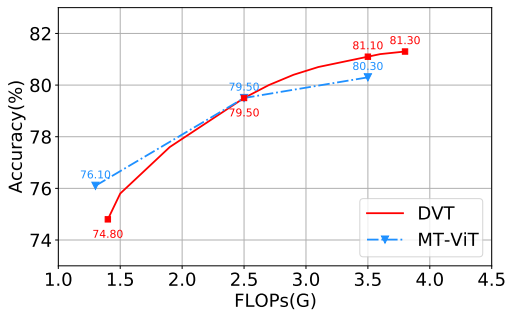


Figure 4: The Accuracy-FLOPs curve of DVT and MT-ViT based on DeiT-S.

Table 6: Comparison results of DVT, MiniViT and MT-ViT, which are implemented on top of DeiT-S.

Method	Param.(M)	Accuracy.(%)	FLOPs(G)
Baseline (DeiT-S)	22M	79.8%	4.6G
DVT	70.4M	79.5% (-0.3%)	2.5G
MT-ViT(S*)	<b>22M+2.5M</b>	79.5% (-0.3%)	2.5G
Mini-DeiT-S	<b>11M</b>	80.0% (+0.2%)	4.6G
MT-ViT(A*)	22M+2.5M	<b>80.3% (+0.5%)</b>	<b>3.5G</b>

Table 7: Performance of MT-ViT when setting different numbers of tokens for different tails.

Method	ST	MT	LT	Top-1 Acc.(%)	Top-5 Acc.(%)	FLOPs(G)
MT-ViT	7×7	10×10	14×14	<b>72.9(+0.7)</b>	<b>91.3(+0.2)</b>	<b>0.8(-38.5%)</b>
	4×4	7×7	14×14	72.4(+0.2)	91.1(+0.0)	0.9(-30.8%)
DeiT-Ti	N/A			72.2	91.1	1.3

tational cost. This is due to the design of MiniViT, which conducts weight sharing strategy to re-use some parameters. But this does not change either the network size or the length of the input sequence. Hence, it cannot accelerate the model for efficient inference. By contrast, the advantage of MT-ViT is that it can greatly reduce the computational cost of ViT. The additional parameters introduced by the predictor and tails are not significant.

### 5.3.6. Number of Tokens for Different Tails

Following DVT’s setting [56], the three tails in MT-ViT are set to output 7×7, 10×10 and 14×14 tokens, respectively. However, the optimal number of tokens for each tail still remains to be explored. As a result, we further investigate how the number of tokens of each tail could influence the performance of MT-ViT. Specifically, a new MT-ViT backbone (based on DeiT-Ti) with 4×4, 7×7 and 14×14 tokens is pre-trained to conduct the experiment. The result is provided in Table 7. MT-ViT backbone with 4×4, 7×7 and 14×14 tokens has a lower computational cost and a relatively lower accuracy. We also observe that MT-ViT with fewer tokens is inferior to MT-ViT with more tokens in both accuracy and FLOPs after the fine-tuning.

### 5.3.7. Predictor backbone

MobileNet-v3-Small [25] is served as the backbone for the tail predictor in the paper due to its low computational cost. However, the lower computational cost may also lead to a worse representation ability and wrong

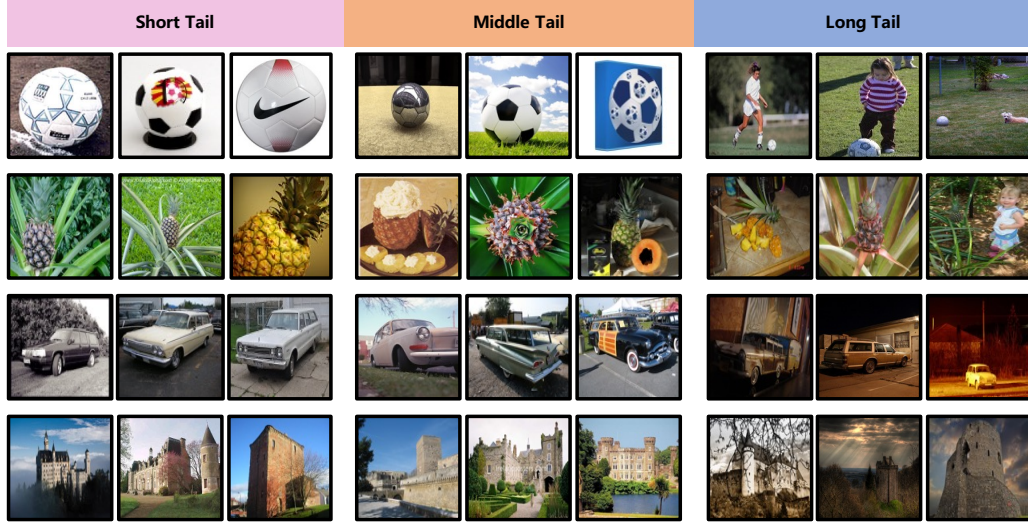


Figure 5: The visualized results of tail predictor in ImageNet-1K. The images in each row are from the class ‘Soccer’, ‘Pineapple’, ‘Car’ and ‘Castle’, respectively. The decision of each tail predictor illustrates how the predictor translates to instance difficulty.

Table 8: Comparison results of different predictor backbones. The resolution is the input size of the tail predictor. The results are based on MT-ViT (DeiT-S).

Backbone	Resolution	FLOPs(G)	Acc.(%)	*FLOPs(G)
MobileNetv3	224×224	0.06	80.3	3.5
ResNet-10	112×112	0.24	80.1	3.5
ResNet-10	224×224	0.89	80.4	4.3

prediction. To find out how the network scale could influence the performance of the tail predictor, we use a relatively large backbone (*i.e.*, ResNet with four basic blocks). The result in Table 8 shows that improving the network scale of the predictor can only slightly improve its prediction, however, it leads to a clear growth on FLOPs. \*FLOPs(G) denotes the summed FLOPs of both the tail predictor and multi-tailed vision transformer backbone. Considering the trade-off between accuracy and FLOPs, we choose to use MobileNet as the backbone of the tail predictor.

#### 5.4. Visualization

To have a better understanding of the role of the tail predictor, we further visualize the decision of the tail predictor on ImageNet-1K, as shown in Figure 8. We choose samples from ImageNet-1K with four categories ‘Soccer’,

‘Pineapple’, ‘Car’, and ‘Castle’ to illustrate how the tail predictor translates instance difficulty. Intuitively, an image with clear and large objects could be identified as an ‘easy’ image, which can also be related to a relatively large prediction confidence of the model. An ‘easy’ image also means that it is simple to be correctly recognized by humans. We hypothesize that decisions of the tail predictor can basically follow the human’s visual judgment. From Figure 8, we can easily observe that the selections of short tail and middle tail are relatively easy to identify since they often have a single frontal view object located in the center of the images. However, the objects in ‘difficult’ images selected by long tail are often blurry and in irregular shape. This confirms our motivation that the tail predictor can measure the instance difficulty. The “sorting” into easy or hard images falls out automatically, which is learned by MT-ViT.

## 6. Conclusion

In this paper, we propose an efficient vision transformer called Multi-Tailed Vision Transformer (MT-ViT) by reducing the number of tokens in the tail of the vision transformer. MT-ViT adopts multiple tails for splitting images into sequences with varying lengths, each of which results in different computational costs and accuracy during inference. We conditionally send images to different tails by introducing a tail predictor that determines which tail is appropriate for the image. During training, the Gumbel-Softmax trick ensures that both modules can be optimized in an end-to-end fashion. The empirical results demonstrate that MT-ViT outperforms baseline and other comparison methods on small-scale datasets (*i.e.*, CIFAR100 and TinyImageNet) and large-scale datasets (*i.e.*, ImageNet-1K). The visualized results of the tail predictor also identify our motivation that the tail predictor can be employed to automatically translate instance difficulty.

## References

- [1] Bakhtiarnia, A., Zhang, Q., Iosifidis, A., 2021. Multi-exit vision transformer for dynamic inference. arXiv preprint arXiv:2106.15183 .
- [2] Brown, T., Mann, B., Ryder, N., Subbiah, M., Kaplan, J.D., Dhariwal, P., Neelakantan, A., Shyam, P., Sastry, G., Askell, A., et al., 2020. Language models are few-shot learners. Advances in neural information processing systems 33, 1877–1901.

- [3] Carion, N., Massa, F., Synnaeve, G., Usunier, N., Kirillov, A., Zagoruyko, S., 2020. End-to-end object detection with transformers, in: European Conference on Computer Vision, Springer. pp. 213–229.
- [4] Chen, C.F.R., Fan, Q., Panda, R., 2021a. Crossvit: Cross-attention multi-scale vision transformer for image classification, in: Proceedings of the IEEE/CVF international conference on computer vision, pp. 357–366.
- [5] Chen, M., Peng, H., Fu, J., Ling, H., 2021b. Autoformer: Searching transformers for visual recognition, in: Proceedings of the IEEE/CVF International Conference on Computer Vision, pp. 12270–12280.
- [6] Chen, T., Cheng, Y., Gan, Z., Yuan, L., Zhang, L., Wang, Z., 2021c. Chasing sparsity in vision transformers: An end-to-end exploration. Advances in Neural Information Processing Systems 34.
- [7] Chopin, B., Tang, H., Otberdout, N., Daoudi, M., Sebe, N., 2023. Interaction transformer for human reaction generation. IEEE Transactions on Multimedia .
- [8] Chrabaszcz, P., Loshchilov, I., Hutter, F., 2017. A downsampled variant of imagenet as an alternative to the cifar datasets. arXiv preprint arXiv:1707.08819 .
- [9] Chu, X., Tian, Z., Wang, Y., Zhang, B., Ren, H., Wei, X., Xia, H., Shen, C., 2021. Twins: Revisiting the design of spatial attention in vision transformers. Advances in Neural Information Processing Systems 34, 9355–9366.
- [10] Deng, J., Dong, W., Socher, R., Li, L.J., Li, K., Fei-Fei, L., 2009. Imagenet: A large-scale hierarchical image database, in: 2009 IEEE conference on computer vision and pattern recognition, Ieee. pp. 248–255.
- [11] Devlin, J., Chang, M.W., Lee, K., Toutanova, K., 2018. Bert: Pre-training of deep bidirectional transformers for language understanding. arXiv preprint arXiv:1810.04805 .
- [12] Dosovitskiy, A., Beyer, L., Kolesnikov, A., Weissenborn, D., Zhai, X., Unterthiner, T., Dehghani, M., Minderer, M., Heigold, G., Gelly, S.,



- et al., 2020. An image is worth 16x16 words: Transformers for image recognition at scale. arXiv preprint arXiv:2010.11929 .
- [13] Fayyaz, M., Koohpayegani, S.A., Jafari, F.R., Sengupta, S., Joze, H.R.V., Sommerlade, E., Pirsiavash, H., Gall, J., 2022. Adaptive token sampling for efficient vision transformers, in: Computer Vision–ECCV 2022: 17th European Conference, Tel Aviv, Israel, October 23–27, 2022, Proceedings, Part XI, Springer. pp. 396–414.
  - [14] Gong, C., Wang, D., Li, M., Chen, X., Yan, Z., Tian, Y., Chandra, V., et al., 2021. Nasvit: Neural architecture search for efficient vision transformers with gradient conflict aware supernet training, in: International Conference on Learning Representations.
  - [15] Goyal, S., Choudhury, A.R., Raje, S., Chakaravarthy, V., Sabharwal, Y., Verma, A., 2020. Power-bert: Accelerating bert inference via progressive word-vector elimination, in: International Conference on Machine Learning, PMLR. pp. 3690–3699.
  - [16] Guo, J., Han, K., Wu, H., Tang, Y., Chen, X., Wang, Y., Xu, C., 2022. Cmt: Convolutional neural networks meet vision transformers, in: Proceedings of the IEEE/CVF Conference on Computer Vision and Pattern Recognition, pp. 12175–12185.
  - [17] Han, K., Wang, Y., Chen, H., Chen, X., Guo, J., Liu, Z., Tang, Y., Xiao, A., Xu, C., Xu, Y., et al., 2020. A survey on visual transformer. arXiv preprint arXiv:2012.12556 .
  - [18] Han, K., Xiao, A., Wu, E., Guo, J., Xu, C., Wang, Y., 2021. Transformer in transformer. Advances in Neural Information Processing Systems 34, 15908–15919.
  - [19] Han, X.F., Jin, Y.F., Cheng, H.X., Xiao, G.Q., 2022. Dual transformer for point cloud analysis. IEEE Transactions on Multimedia .
  - [20] He, K., Zhang, X., Ren, S., Sun, J., 2016. Deep residual learning for image recognition, in: Proceedings of the IEEE conference on computer vision and pattern recognition, pp. 770–778.
  - [21] He, S., Luo, H., Wang, P., Wang, F., Li, H., Jiang, W., 2021. Transreid: Transformer-based object re-identification, in: Proceedings of

- the IEEE/CVF international conference on computer vision, pp. 15013–15022.
- [22] He, Y., Zhang, X., Sun, J., 2017. Channel pruning for accelerating very deep neural networks, in: Proceedings of the IEEE international conference on computer vision, pp. 1389–1397.
  - [23] Heo, B., Yun, S., Han, D., Chun, S., Choe, J., Oh, S.J., 2021. Rethinking spatial dimensions of vision transformers, in: Proceedings of the IEEE/CVF International Conference on Computer Vision, pp. 11936–11945.
  - [24] Hinton, G., Vinyals, O., Dean, J., 2015. Distilling the knowledge in a neural network. arXiv preprint arXiv:1503.02531 .
  - [25] Howard, A., Sandler, M., Chu, G., Chen, L.C., Chen, B., Tan, M., Wang, W., Zhu, Y., Pang, R., Vasudevan, V., et al., 2019. Searching for mobilenetv3, in: Proceedings of the IEEE/CVF international conference on computer vision, pp. 1314–1324.
  - [26] Jang, E., Gu, S., Poole, B., 2016. Categorical reparameterization with gumbel-softmax. arXiv preprint arXiv:1611.01144 .
  - [27] Jia, M., Cheng, X., Lu, S., Zhang, J., 2022. Learning disentangled representation implicitly via transformer for occluded person re-identification. IEEE Transactions on Multimedia .
  - [28] Jiang, Y., Chang, S., Wang, Z., 2021a. Transgan: Two pure transformers can make one strong gan, and that can scale up. Advances in Neural Information Processing Systems 34.
  - [29] Jiang, Z.H., Hou, Q., Yuan, L., Zhou, D., Shi, Y., Jin, X., Wang, A., Feng, J., 2021b. All tokens matter: Token labeling for training better vision transformers. Advances in Neural Information Processing Systems 34, 18590–18602.
  - [30] Jiao, J., Tang, Y.M., Lin, K.Y., Gao, Y., Ma, J., Wang, Y., Zheng, W.S., 2023. Dilateformer: Multi-scale dilated transformer for visual recognition. IEEE Transactions on Multimedia .

- [31] Krizhevsky, A., Hinton, G., et al., 2009. Learning multiple layers of features from tiny images .
- [32] Krizhevsky, A., Sutskever, I., Hinton, G.E., 2012. Imagenet classification with deep convolutional neural networks. *Advances in neural information processing systems* 25, 1097–1105.
- [33] Lee, K., Chang, H., Jiang, L., Zhang, H., Tu, Z., Liu, C., 2021. Vitgan: Training gans with vision transformers, in: *International Conference on Learning Representations*.
- [34] Liang, Y., Chongjian, G., Tong, Z., Song, Y., Wang, J., Xie, P., 2021. Evit: Expediting vision transformers via token reorganizations, in: *International Conference on Learning Representations*.
- [35] Liang, Y., Ge, C., Tong, Z., Song, Y., Wang, J., Xie, P., 2022. Not all patches are what you need: Expediting vision transformers via token reorganizations. *arXiv preprint arXiv:2202.07800* .
- [36] Liu, Z., Li, J., Shen, Z., Huang, G., Yan, S., Zhang, C., 2017. Learning efficient convolutional networks through network slimming, in: *Proceedings of the IEEE international conference on computer vision*, pp. 2736–2744.
- [37] Liu, Z., Lin, Y., Cao, Y., Hu, H., Wei, Y., Zhang, Z., Lin, S., Guo, B., 2021. Swin transformer: Hierarchical vision transformer using shifted windows, in: *Proceedings of the IEEE/CVF International Conference on Computer Vision*, pp. 10012–10022.
- [38] Maddison, C.J., Mnih, A., Teh, Y.W., 2016. The concrete distribution: A continuous relaxation of discrete random variables. *arXiv preprint arXiv:1611.00712* .
- [39] Pan, B., Panda, R., Jiang, Y., Wang, Z., Feris, R., Oliva, A., 2021a. Ia-red2: Interpretability-aware redundancy reduction for vision transformers. *Advances in Neural Information Processing Systems* 34.
- [40] Pan, Z., Zhuang, B., Liu, J., He, H., Cai, J., 2021b. Scalable vision transformers with hierarchical pooling, in: *Proceedings of the IEEE/cvf international conference on computer vision*, pp. 377–386.

- [41] Peng, H., Du, H., Yu, H., Li, Q., Liao, J., Fu, J., 2020. Cream of the crop: Distilling prioritized paths for one-shot neural architecture search. *Advances in Neural Information Processing Systems* 33, 17955–17964.
- [42] Qiu, Z., Qiu, K., Fu, J., Fu, D., 2020. DgcN: Dynamic graph convolutional network for efficient multi-person pose estimation, in: *Proceedings of the AAAI Conference on Artificial Intelligence*, pp. 11924–11931.
- [43] Qiu, Z., Yang, H., Fu, J., Fu, D., 2022a. Learning spatiotemporal frequency-transformer for compressed video super-resolution, in: *European Conference on Computer Vision*, Springer. pp. 257–273.
- [44] Qiu, Z., Yang, Q., Wang, J., Fu, D., 2022b. Ivt: An end-to-end instance-guided video transformer for 3d pose estimation, in: *Proceedings of the 30th ACM International Conference on Multimedia*, pp. 6174–6182.
- [45] Rao, Y., Zhao, W., Liu, B., Lu, J., Zhou, J., Hsieh, C.J., 2021. Dynamicvit: Efficient vision transformers with dynamic token sparsification. *Advances in neural information processing systems* 34, 13937–13949.
- [46] Srinivas, A., Lin, T.Y., Parmar, N., Shlens, J., Abbeel, P., Vaswani, A., 2021. Bottleneck transformers for visual recognition, in: *Proceedings of the IEEE/CVF Conference on Computer Vision and Pattern Recognition*, pp. 16519–16529.
- [47] Sun, C., Shrivastava, A., Singh, S., Gupta, A., 2017. Revisiting unreasonable effectiveness of data in deep learning era, in: *Proceedings of the IEEE international conference on computer vision*, pp. 843–852.
- [48] Tan, M., Le, Q., 2019. Efficientnet: Rethinking model scaling for convolutional neural networks, in: *International Conference on Machine Learning*, PMLR. pp. 6105–6114.
- [49] Tang, W., He, F., Liu, Y., 2022a. Ydtr: infrared and visible image fusion via y-shape dynamic transformer. *IEEE Transactions on Multimedia* .
- [50] Tang, Y., Han, K., Wang, Y., Xu, C., Guo, J., Xu, C., Tao, D., 2022b. Patch slimming for efficient vision transformers, in: *Proceedings of the IEEE/CVF Conference on Computer Vision and Pattern Recognition*, pp. 12165–12174.

- [51] Tang, Y., Wang, Y., Xu, Y., Tao, D., Xu, C., Xu, C., Xu, C., 2020. Scop: Scientific control for reliable neural network pruning. *Advances in Neural Information Processing Systems* 33, 10936–10947.
- [52] Touvron, H., Cord, M., Douze, M., Massa, F., Sablayrolles, A., Jégou, H., 2021. Training data-efficient image transformers & distillation through attention, in: *International Conference on Machine Learning*, PMLR. pp. 10347–10357.
- [53] Vaswani, A., Shazeer, N., Parmar, N., Uszkoreit, J., Jones, L., Gomez, A.N., Kaiser, Ł., Polosukhin, I., 2017. Attention is all you need, in: *Advances in neural information processing systems*, pp. 5998–6008.
- [54] Wang, W., Xie, E., Li, X., Fan, D.P., Song, K., Liang, D., Lu, T., Luo, P., Shao, L., 2021a. Pyramid vision transformer: A versatile backbone for dense prediction without convolutions, in: *Proceedings of the IEEE/CVF International Conference on Computer Vision*, pp. 568–578.
- [55] Wang, W., Yao, L., Chen, L., Lin, B., Cai, D., He, X., Liu, W., 2021b. Crossformer: A versatile vision transformer hinging on cross-scale attention, in: *International Conference on Learning Representations*.
- [56] Wang, Y., Huang, R., Song, S., Huang, Z., Huang, G., 2021c. Not all images are worth 16x16 words: Dynamic transformers for efficient image recognition. *Advances in Neural Information Processing Systems* 34, 11960–11973.
- [57] Wang, Y., Wang, X., Dinh, A.D., Du, B., Xu, C., 2023. Learning to schedule in diffusion probabilistic models, in: *Proceedings of the 29th ACM SIGKDD Conference on Knowledge Discovery and Data Mining*.
- [58] Wang, Y., Xu, C., Du, B., 2021d. Robust adversarial imitation learning via adaptively-selected demonstrations., in: *IJCAI*, pp. 3155–3161.
- [59] Wang, Y., Xu, C., Du, B., Lee, H., 2021e. Learning to weight imperfect demonstrations, in: *International Conference on Machine Learning*, PMLR. pp. 10961–10970.
- [60] Wu, K., Peng, H., Chen, M., Fu, J., Chao, H., 2021. Rethinking and improving relative position encoding for vision transformer, in: *Proceedings of the IEEE/CVF International Conference on Computer Vision*, pp. 10033–10041.

- [61] Wu, K., Zhang, J., Peng, H., Liu, M., Xiao, B., Fu, J., Yuan, L., 2022. Tinyvit: Fast pretraining distillation for small vision transformers, in: European Conference on Computer Vision, Springer. pp. 68–85.
- [62] Xu, R., Liu, Z., Luo, Y., Hu, H., Shen, L., Du, B., Kuang, K., Yang, J., 2023. Sgda: Towards 3d universal pulmonary nodule detection via slice grouped domain attention. *IEEE/ACM Transactions on Computational Biology and Bioinformatics* .
- [63] Xu, R., Luo, Y., Du, B., Kuang, K., Yang, J., 2022a. Lssanet: A long short slice-aware network for pulmonary nodule detection, in: International Conference on Medical Image Computing and Computer-Assisted Intervention, Springer. pp. 664–674.
- [64] Xu, Y., Zhang, Z., Zhang, M., Sheng, K., Li, K., Dong, W., Zhang, L., Xu, C., Sun, X., 2022b. Evo-vit: Slow-fast token evolution for dynamic vision transformer, in: Proceedings of the AAAI Conference on Artificial Intelligence, pp. 2964–2972.
- [65] Xue, Z., Tan, X., Yu, X., Liu, B., Yu, A., Zhang, P., 2022. Deep hierarchical vision transformer for hyperspectral and lidar data classification. *IEEE Transactions on Image Processing* 31, 3095–3110.
- [66] Yin, H., Vahdat, A., Alvarez, J.M., Mallya, A., Kautz, J., Molchanov, P., 2022. A-vit: Adaptive tokens for efficient vision transformer, in: Proceedings of the IEEE/CVF Conference on Computer Vision and Pattern Recognition, pp. 10809–10818.
- [67] Yu, H., Peng, H., Huang, Y., Fu, J., Du, H., Wang, L., Ling, H., 2022. Cyclic differentiable architecture search. *IEEE Transactions on Pattern Analysis and Machine Intelligence* .
- [68] Yuan, L., Chen, Y., Wang, T., Yu, W., Shi, Y., Jiang, Z.H., Tay, F.E., Feng, J., Yan, S., 2021. Tokens-to-token vit: Training vision transformers from scratch on imagenet, in: Proceedings of the IEEE/CVF International Conference on Computer Vision, pp. 558–567.
- [69] Zhang, J., Peng, H., Wu, K., Liu, M., Xiao, B., Fu, J., Yuan, L., 2022. Minivit: Compressing vision transformers with weight multiplexing, in: Proceedings of the IEEE/CVF Conference on Computer Vision and Pattern Recognition, pp. 12145–12154.

- [70] Zhao, J., Wang, H., Zhou, Y., Yao, R., Chen, S., El Saddik, A., 2022. Spatial-channel enhanced transformer for visible-infrared person re-identification. *IEEE Transactions on Multimedia* .
- [71] Zhou, D., Kang, B., Jin, X., Yang, L., Lian, X., Jiang, Z., Hou, Q., Feng, J., 2021. Deepvit: Towards deeper vision transformer. *arXiv preprint arXiv:2103.11886* .